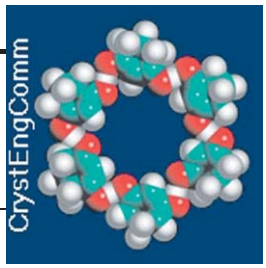

Paper

Synthesis, crystal structure and magnetic properties of two-dimensional malonato-bridged cobalt(II) and nickel(II) compounds

Fernando S. Delgado,[a] María Hernández-Molina,[a] Joaquín Sanchiz,[c] Catalina Ruiz-Pérez,*[a] Yolanda Rodríguez-Martín,[a] Trinidad López,[b] Francesc Lloret[d] and Miguel Julve[d]

[a]*Laboratorio de Rayos X y Materiales Moleculares, Departamento de Física Fundamental II, Universidad de La Laguna., Tenerife, Spain. E-mail: caruiz@ull.es; Fax: (+34) 922 318320; Tel: (+34) 922318236*

[b]*Grupo de Crecimiento Cristalino, Departamento de Física Básica, Universidad de La Laguna, Avda. Astrofísico Francisco Sánchez s/n, 38204 La Laguna, Tenerife, Spain*

[c]*Departamento de Química Inorgánica, Universidad de La Laguna, 38204 La Laguna, Tenerife, Spain*

[d]*Departament de Química Inorgànica/Instituto de Ciencia Molecular, Facultat de Química, Universitat de València, Avda. Dr. Moliner 50, 46100 Burjassot, València, Spain*

Received 9th March 2004, Accepted 23rd March 2004
First published as an Advance Article on the web 5th April 2004

Two isostructural malonato-bridged complexes of formula $\{[M(H_2O)_2][M(mal)_2(H_2O)_2]\}_n$ [M = Co(II) (**1**), Ni(II) (**2**); H_2mal = malonic acid] have been synthesised and characterized by X-ray diffraction. Their structure consists of corrugated layers of *trans*-diaquabismalonatemetalate(II) and *trans*-diaquametal(II) units bridged by carboxylate–malonate groups in the *anti–syn* conformation. Two crystallographycally independent metal atoms occur in **1** and **2**. The malonate anion acts simultaneously as a bidentate and bis-monodentate ligand. Variable-temperature (1.9–295 K) magnetic susceptibility measurements indicate the occurrence of weak antiferro- (**1**) and ferromagnetic (**2**) interactions between the cobalt(II) (**1**) and nickel(II) ions (**2**) through the *anti–syn* caboxylate–malonate bridge. A brief discussion on the structural diversity and crystal engineering possibilities of the malonate complexes with divalent first-row transition metal ions other than copper(II) is carried out.

Introduction

There has been an increasing interest in complexes containing paramagnetic metal ions exhibiting extended networks because of their potential applications in molecular magnetic materials.[1] The ability of the bridging ligand to mediate magnetic coupling between the paramagnetic centers that it links plays a fundamental role in these studies, as shown by the oxalato,[2,3] cyano,[3,4] azide,[5] oximato[6] or dicyanamide[7] ligands. The malonate group (the dianion of 1,3-propanedioic acid, H_2mal) is a suitable candidate in designing extended magnetic networks because it has been proved to be a very versatile ligand in crystal engineering and in materials science.[8–10] The occurrence of two carboxylate groups in 1,3-positions allows this ligand to adopt several coordination modes. A great variety of crystal structures ranging from mononuclear species[11,12] to three-dimensional networks[13–17] can be built with the malonate ligand depending on the metal ions it bridges and on the presence of coligands.

Let us focus on the homometallic complexes with first-row transition metal ions that only contain malonate and water as ligands. Different topologies have been observed for the structures of the copper(II) complexes, their nuclearity ranging from discrete entities[11,18,19] to chain compounds.[18] Most of these complexes have been magnetically characterized and they exhibit ferromagnetic coupling through the carboxylate–malonate bridge.[18] On the other hand, two-dimensional structures with different topologies have been reported for the malonate complexes with zinc(II)[20] and manganese(II)[21] ions. An overall weak antiferromagnetic coupling and a spin-canting behaviour at very low temperature (T_c = 2.7 K) have been observed for the manganese(II) compound.[13] No single crystals of the malonate-containing nickel(II) and cobalt(II) complexes are available but the analysis of their X-ray powder diffraction data reveal that they are isostructural with the zinc(II) malonate.[22]

In the framework of our magneto-structural studies on malonate-containing metal complexes, we got single crystals of the two-dimensional compounds $\{[M(H_2O)_2][M(mal)_2(H_2O)_2]\}_n$ with M = Co(II) (**1**) and Ni(II) (**2**). We report here their preparation, crystal structure determination and magnetic characterization together with a brief discussion of the structural possibilities offered by this family of homometallic two-dimensional malonato complexes.

Experimental

Materials and methods

Malonic acid, cobalt(II) acetate tetrahydrate and nickel(II) acetate tetrahydrate were purchased from Aldrich and used as received. Elemental analyses (C, H) were performed on a EA 1108 CHNS-O microanalytical analyzer. IR spectra (450–4000 cm^{-1}) were recorded on a Brüker IF S55 spectrophotometer with the samples prepared as KBr pellets. Magnetic susceptibility measurements on polycrystalline samples of compounds **1** and **2** were carried out in the temperature range 1.9–295 K with a Quantum Design SQUID magnetometer. The applied magnetic field was 1 T for $T \geqslant 100$ K and 250 Oe for $T < 100$ K in order to avoid saturation phenomena.

 DOI: 10.1039/b403640a

Diamagnetic corrections for the constituent atoms were estimated from Pascal's constants[23] as -156×10^{-6}, and -160×10^{-6} cm^3 mol^{-1} for compounds **1** and **2**, respectively. Experimental susceptibilities were also corrected for the temperature-independent paramagnetism [100×10^{-6} cm^3 mol^{-1} per Ni(II) ion] and the magnetization of the sample holder.

Synthesis

$\{[Co(H_2O)_2][Co(mal)_2(H_2O)_2]\}_n$ (1). Malonic acid (11 mmol, 1.14 g) is added to an aqueous solution (100 cm^3) of cobalt(II) acetate (10 mmol, 2.49 g) under continuous stirring. The volume of the resulting solution is reduced to *ca.* 50 cm^3 by heating in a steam bath at 60 °C in order to evaporate the acetic acid. Single crystals of **1** as red prisms were grown on standing by keeping the temperature of steam bath at *ca.* 40 °C. Yield: 75%. Anal. Calcd. for $C_6O_{12}H_{12}Co_2$: C, 18.28; H, 3.00. Found: C, 18.35; H, 3.10%. Selected IR peaks (KBr/cm^{-1}): *ν*(COO) 1663, 1581sh, 1565, 1451, 1373, 721.

$\{[Ni(H_2O)_2][Ni(mal)_2(H_2O)_2]\}_n$ (2). X-ray quality crystals of **2** as green needles were prepared by following the procedure detailed above for **1** but using nickel(II) acetate instead of the cobalt(II) one. Yield: 65%. Anal. Calcd. for $C_6O_{12}H_{12}Ni_2$: C, 18.30; H, 3.0. Found: C, 18.22; H, 3.12%. Selected IR peaks (KBr/cm^1): *ν*(COO) 1665, 1585sh, 1567, 1453, 1376, 726.

Crystal data collection and refinement

Single crystals of **1** and **2** were mounted on a Bruker–Nonius KappaCCD diffractometer. Orientation matrix and lattice parameters were obtained by least-squares refinement of the reflections obtained by a θ–χ scan (Dirax/lsq method). Diffraction data of **1** and **2** were collected at 293(2) K using graphite-monochromated Mo Kα radiation ($\lambda = 0.71073$ Å). A summary of the crystallographic data and structure refinement is given in Table 1. The indexes of data collection were $-15 \leqslant h \leqslant 16$, $-9 \leqslant k \leqslant 8$, $-9 \leqslant l \leqslant 7$ for **1** and $-17 \leqslant h \leqslant 10$, $-8 \leqslant k \leqslant 10$, $-10 \leqslant l \leqslant 10$ for **2**. Of the 723 (**1**) and 887 (**2**) measured independent reflections in the θ range 5.25–27.5° (**1**) and 6.43–30° (**2**), 612 (**1**) and 637 (**2**) have $I \geqslant 2\sigma(I)$. All the measured independent reflections were used in the analysis. All calculations for data reduction, structure solution, and refinement were done by standard procedures (WINGX).[24] The structure was solved by direct methods and refined with full-matrix least-squares technique on F^2 using the SHELXS-97[25] and SHELXL-97[25] programs. In both compounds the malonate hydrogen atoms were located from difference Fourier maps and refined with isotropic temperature factors. The hydrogen atoms of the water molecules were not found. The final Fourier-difference map showed maximum and minimum height peaks of 0.661 and -0.450 e Å^{-3} for **1** and of 0.682 and -0.539 e Å^{-3} for **2**. The final geometrical calculations and the graphical manipulations were carried out with PARST97[26] and CRYSTAL MAKER[27] programs, respectively. Selected bond distances and angles for **1** and **2** are listed in Table 2.

For cobalt(II) and nickel(II) malonates[22] CCSD reference codes are QQQFRA and QQQFRD, respectively.

CCDC reference numbers 231721 (**1**) and 231722 (**2**).

See http://www.rsc.org/suppdata/ce/b4/b403640a/ for crystallographic data in CIF format.

Table 1 Crystal data and details of structure determination

Compound	**1**	**2**
Formula	$C_3H_6CoO_6$	$C_3H_6NiO_6$
M	197.01	196.79
Crystal system	Monoclinic	Monoclinic
Space group	*C*2/*m*	*C*2/*m*
a/Å	12.646(3)	12.5748(5)
b/Å	7.4040(10)	7.3781(6)
c/Å	7.2970(10)	7.2274(4)
α/°	90.0	90.0
β/°	120.18(3)	120.391(6)
γ/°	90.0	90.0
V/Å^3	590.61(2)	578.41(6)
Z	4	4
T/K	293(2)	293(2)
ρ_{calc}/Mg m^{-3}	2.216	2.260
λ (Mo K$_\alpha$ Å)	0.71073	0.71073
μ (Mo–Kα)/mm^{-1}	2.874	3.322
R_1, $I > 2\sigma(I)$ (all)	0.026 (0.034)	0.042 (0.071)
wR_2, $I > 2\sigma(I)$ (all)	0.076 (0.079)	0.086 (0.092)
Measured reflections	1572	1943
Independent reflections (R_{int})	723 (0.016)	887 (0.042)

Results and discussion

Description of the structures of 1 and 2

Complexes **1** and **2** are isostructural compounds. Their structure consists of corrugated layers containing $[M(1)(mal)_2(H_2O)_2]^{2-}$ anions and $[M(2)(H_2O)_2]^{2+}$ cations with M(1) = M(2) = Co(II) (**1**) and Ni(II) (**2**) which are linked by carboxylate-malonate groups in the *anti-syn* bridging mode (Fig. 1a). These layers grow in the *bc*-plane and they exhibit intralayer [between O(2w) and the O(1) and O(1f) malonate-oxygen atoms] and interlayer [between O(1w) and the O(2g) and O(2h) malonate oxygens] hydrogen bonds [see Table 3 and Fig. 1b], the latter ones leading to a three-dimensional structure.

There are two crystallographically independent metal ions [M(1) and M(2)] which lie on a 2/*m* crystallographic site (Fig. 2). Both metal ions are six-coordinated in slightly distorted octahedral environments: they have in common the occurrence of two *trans* coordinated water molecules in the apical positions and four oxygen atoms from two [at M(1)] and four [at M(2)] malonate ligands in the equatorial plane. Some characteristic geometric values[28] for **1** and **2** are listed in Table 4. The equatorial M(1)–O bond distances [2.050(2) and 2.021(2) Å for **1** and **2**, respectively] are somewhat shorter than the apical ones [2.123(3) (**1**) and 2.090(4) Å (**2**)], leading to an elongated distorted octahedral environment around M(1). The opposite trend is observed at M(2) whose octahedral environment is axially compressed, the values of the equatorial M(2)–O bond distances [2.119(2) Å (**1**) and 2.087(2) Å (**2**)] being longer than the apical ones [2.081(2) Å (**1**) and 2.058(3) Å (**2**)]. All geometric values are in good agreement with those observed in the isostructural zinc(II) malonate.[20]

The methylene–malonate group lies on a crystallographic mirror plane. Each malonate ligand adopts simultaneously the bidentate [through O(1) and O(1a) toward M(1)] and bis-monodentate [through O(3) and O(3a) toward M(2) and

Table 2 Selected bond lengths (Å) and angles (°) for compounds **1** and **2**[a]

Compound	**1**	**2**
M(1)–O(1)	2.050(2)	2.021(2)
M(1)–O(1w)	2.123(3)	2.090(4)
M(2)–O(2)	2.119(2)	2.087(2)
M(2)–O(2w)	2.081(2)	2.058(3)
O(1)–M(1)–O(1a)	89.52(10)	90.55(13)
O(1)–M(1)–O(1c)	90.48(10)	89.45(13)
O(1)–M(1)–O(1w)	91.85(8)	92.20(10)
O(1)–M(1)–O(1wc)	88.15(8)	87.80(10)
O(2)–M(2)–O(2d)	86.45(11)	86.76(14)
O(2)–M(2)–O(2f)	93.55(11)	93.24(14)
O(2)–M(2)–O(2w)	93.45(7)	93.92(9)
O(2)–M(2)–O(2wd)	86.55(7)	86.08(9)

[a] Symmetry code: (a) $x, -y, z$; (b) $1-x, -y, 1-z$; (c) $1-x, y, 1-z$; (d) $1-x, y, 2-z$; (e) $1-x, 1-y, 2-z$; (f) $x, 1-y, z$.

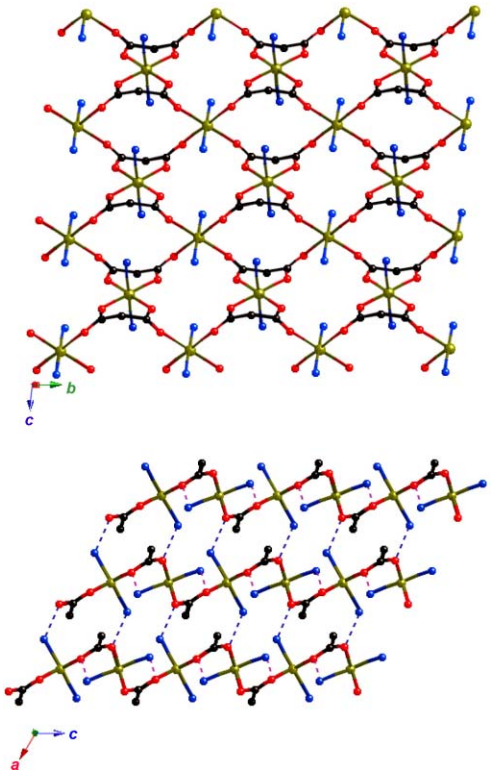

Fig. 1 (a) Perspective view of a fragment of the corrugated malonate-bridged layer of **1** [M = Co(II)] and **2** [M = Ni(II)] growing in the *bc* plane. Click here to access a 3D view of Fig. 1a. (b) Side view of three adjacent layers of **1** and **2** showing the intra- and interlayer hydrogen bonds (broken lines).

Table 3 Relevant H-bond distances for compounds **1** and **2**[a]

Compound	1	2
D···A		
Intralayer		
O(2w)···O(1)	2.680(2)	2.673(3)
O(2w)···O(1f)	2.680(2)	2.673(3)
Interlayer		
O(1w)···O(2g)	2.860(4)	2.853(5)
O(1w)···O(2h)	2.860(4)	2.853(5)

[a] Symmetry code: (f) x, $1 - y$, z; (g) $1/2 - x$, $1/2 - y$, $1 - z$; (h) $1/2 - x$, $-1/2 + y$, $1 - z$

M(2a)] coordination modes and exhibits an envelope conformation (see geometric values[29] in Table 4). The carboxylate–malonate groups exhibit the *anti–syn* conformation and they connect two equatorial positions of the M(1) and M(2) metal ions. The values of the C–C [1.516(3) Å and 1.518(4) Å for **1** and **2**, respectively] and C–O [1.249(3)–1.263(3) (**1**) and 1.253(4)–1.262(4) Å (**2**)] malonate bond distances and O–C–O [123.0(2)° (**1**) and 123.1(3)° (**2**)] bond angles agree well with those previously reported in other malonate-containing complexes.[13,14,17,20,21,30–35]

Each M(1) atom is connected to four M(2) atoms through *anti–syn* carboxylate groups from two malonate ligands to afford corrugated layers. The two crystallographically independent metal atoms [M(1) and M(2)] are set in the same plane within each layer, whereas the malonate ligands are shifted from these metal planes. The values of the dihedral angles between the equatorial plane of the M(1) and M(2) atoms and the O(1)–C(1)–O(2) mean plane are 22.6(2) and 77.64(13)° for **1** and 22.5(3) and 77.2(2)° for **2**. The equatorial planes of M(1) and M(2) form dihedral angles of 79.45(4)° (**1**) and 80.17(6)° (**2**). The values of the shortest intra- and interlayer metal–metal distances are listed in Table 5.

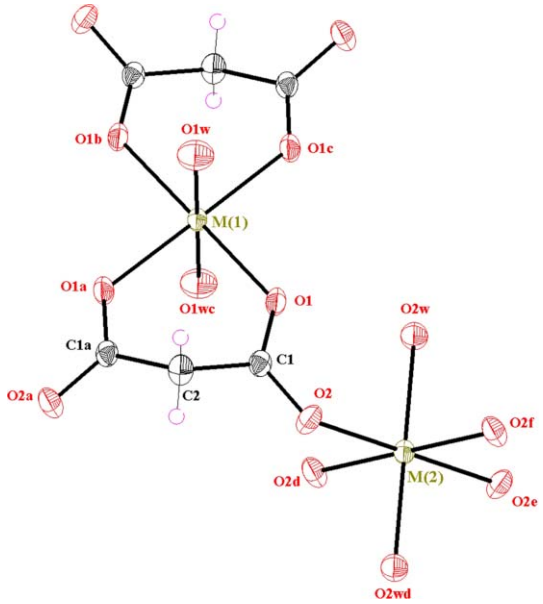

Fig. 2 Perspective view showing the two crystallographically independent metal ions in **1** [M = Co(II)] and **2** [M = Ni(II)]. Thermal ellipsoids are drawn at the 50% probability level and they correspond to **1**.

Table 4 Geometric values for compounds **1** and **2**[a]

Compound	1	2
Geometric values for metal environment around M(1)		
s/h	1.247	1.246
Φ/°	58.8	56.9
Geometric values for metal environment around M(2)		
s/h	1.230	1.214
Φ/°	61.32	64.97
Ring puckering parameters (chelating malonate)		
Phase angle, ϕ/°	120.0(3)	120.0(4)
θ/°	73.2(2)	74.4(3)
Total puckering amplitude, Q_T	0.461(3)	0.451(5)

[a] See refs. 28 and 29.

Influence of the coligand on the structure of the homometallic malonate complexes

Let us carry out a brief survey of the structural possibilities of the homometallic malonate complexes in the presence of a coligand. The structures of the hydrated phases of the manganese(II) and zinc(II) malonate complexes were previously described by Lys *et al.*[21] and Ray *et al.*,[20] respectively. The structure of these compounds consists basically of layers of malonate-containing transition metal ions (see Scheme 1, top). In the case of manganese(II) the layers are built of *trans*-diaquamanganese(II) units bridged by carboxylate–malonate groups in the *anti–syn* and *anti–anti* bridging modes [intralayer Mn···Mn separations through the *anti–anti* and the *anti–syn* carboxylate bridges

Table 5 Values of the shortest metal–metal separations in compounds **1** and **2**[a]

Compound	1	2
Intralayer		
M(1)···M(2)	5.1977(5)	5.1641(3)
M(1)···M(1i)	7.4040(10)	7.3781(6)
M(2)···M(2j)	7.2970(10)	7.2274(4)
Interlayer		
M(1)···M(2k)	5.486(2)	5.4407(4)

[a] Symmetry code: (i) x, $y + 1$, z; (j) x, y, $z - 1$; (k) $1/2 + x$, $-1/2 + y$, z.

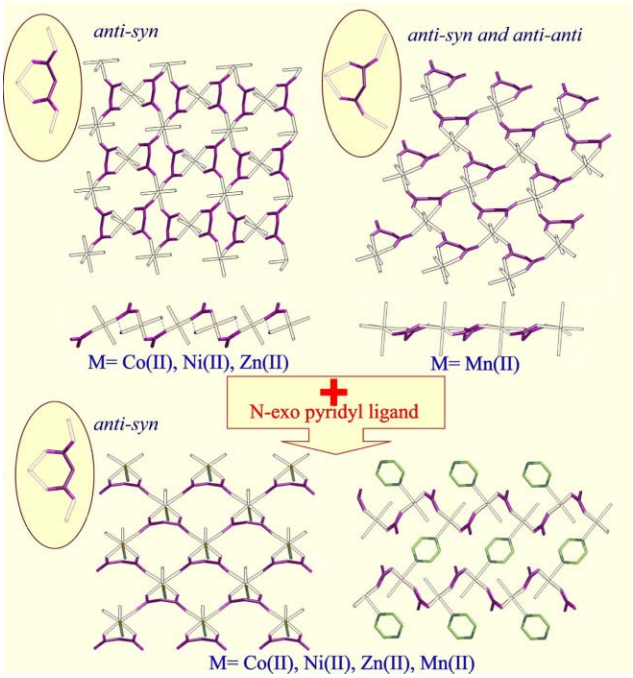

Scheme 1

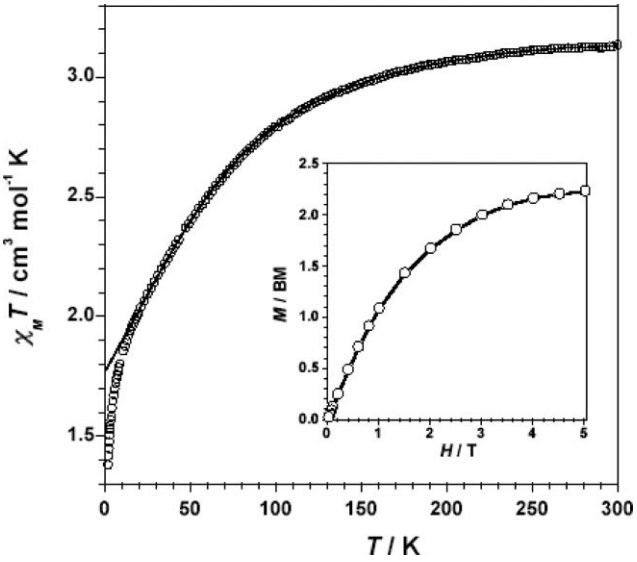

Fig. 3 Thermal dependence of the $\chi_M T$ product for **1** per Co: (○) experimental; (—) best-fit curve (see text). The inset shows the magnetisation *versus* H plot at 2.0 K for **1**: (○) experimental; (—) eye-guide line.

being 5.790(4) and 6.319(4) Å, respectively]. The malonate groups do not deviate significantly from the plane defined by metal ions. On the other hand, two crystallographically independent metal ions are present in the isostructural zinc(II), cobalt(II) (**1**) and nickel(II) (**2**) malonate series. These three compounds have also a two-dimensional structure with *trans*-diaquabismalonatemetalate(II) and *trans*-diaquametal(II) units being bridged through *anti–syn* carboxylate–malonate groups [intralayer M···M separation ranging from 5.1566(5) to 5.2072(7) Å]. In contrast to the planar manganese(II) malonate structure, the layers in this series are corrugated, the malonate ligands within each layer being out of the plane defined by the metal ions. In all homometallic malonate compounds with divalent first-row transition metal ions, hydrogen bonds involving coordinated water molecules and malonate oxygen atoms contribute to stabilizing the crystal structure and lead to a three-dimensional network.

Although the homometallic malonate complexes have significant structural differences, when they react with N-exo pyridyl ligands such as pyrimidine (pym), pyrazine (pyz), 2,4′-bipyridine (2,4′-bpy) and 4,4′-bipyridine (4,4′-bpy), the layer containing the malonate and the metal ions is kept, the N-donor atom of the pyridyl ligand occupying an apical position of the metal environment for M = Mn(II),[13,31] Co(II),[14,17,35] Zn(II),[17,33,34] and Ni(II).[36] The topology of these layers (Scheme 1, bottom) is different from those of the diaquamalonatemetal(II) ones (Scheme 1, top). Aquametal(II) units linked by carboxylate–malonate groups in the *anti–syn* bridging mode build the corrugated layer in the complexes containing the N-donor. Additionally, weak π–π stacking interactions between pyridyl-rings in this family can contribute to the stabilization of the resulting network.

Several malonate complexes have been reported with other N-donor ligands. The reaction of manganese(II) malonate complexes with chelating ligands such as 2,2′-bipyridine (2,2′-bpy)[32] and 1,10-phenantroline (phen)[30] afforded mononuclear neutral units which are linked by hydrogen bonds into 3-D networks. Finally, the reaction of Co(II) malonate with hexamethylenetetramine (urotropine)[14] and benzimidazole[37,38] yielded monomeric entities and two- and three-dimensional structures where corrugated layers of malonate-bridged cobalt(II) ions are present.

Magnetic properties of 1 and 2

The thermal dependence of the $\chi_M T$ product [χ_M being the magnetic susceptibility per cobalt(II) ion] for compound **1** is shown in Fig. 3. At room temperature, $\chi_M T$ is equal to 3.12 cm^3 mol^{-1} K, a value which is greater than that expected for the spin-only one for a high spin cobalt(II) ion (1.87 cm^3 mol^{-1} K with $g = 2.0$). This is due to the occurrence of an unquenched orbital contribution typical of the $^4T_{1g}$ ground state in six-coordinated cobalt(II) complexes.[39,40] Upon cooling, $\chi_M T$ continuously decreases reaching a minimum value of 1.35 cm^3 mol^{-1} K at 2.0 K. No maximum of susceptibility is observed in the χ_M *versus* T plot. The decrease of $\chi_M T$ with T can be due to depopulation of the higher energy Kramers doublets of cobalt(II) and/or to antiferromagnetic interactions. In this respect, the carboxylate group is known to play the role of antiferromagnetic coupler in carboxylate-bridged cobalt(II) complexes,[17,41–43] the values of the exchange coupling (J) ranging from −3 to −1 cm^{-1}. Thus, having in mind that the magnetic interactions in **1** are most likely very weak, its magnetic behaviour would be monitored by spin–orbit coupling effects. In order to test this assumption, and taking into account that the two crystallographically independent six-coordinated cobalt(II) ions are axially distorted (four carboxylate malonate and two water molecules in *trans* positions), we have analyzed the magnetic data of **1** through the Hamiltonian of eqn. (1)[44]

$$\boldsymbol{H} = -A\kappa\lambda\boldsymbol{LS} + D[\boldsymbol{L}_z^2 - (1/3)L(L+1)] + \beta(-A\kappa\boldsymbol{L} + g_e\boldsymbol{S})H \quad (1)$$

where spin–orbit coupling (first term), axial distortion (second term) and Zeeman interaction (last term) are considered. No analytical expression for the magnetic susceptibility as a function of A, κ, λ and D can be derived and the values of these parameters were determined by matrix diagonalization. Taking into account that a value of $A = 3/2$ is used in most of the studies with Co(II) where the weak crystal field is involved (as in **1**) and in order to avoid the overparametrization, we introduced a fixed value of 1.5 for A in the fitting procedure. Best-fit parameters of the experimental data of **1** for $T > 15$ K are: $A = 1.5$ (fixed), $\kappa = 0.98$, $\lambda = -137$ cm^{-1} and $D = 506$ cm^{-1}. The calculated curve reproduces very well the experimental data in the temperature range 15–300 K and the

computed values are within the range of those reported for high spin cobalt(II) in the literature. When $T < 15$ K, the magnetic data of Fig. 3 are below the calculated curve indicating that a weak antiferromagnetic interaction between the cobalt(II) ions occurs. An inspection of the structure of **1** shows that the exchange pathways for these interactions are provided by intra- and interlayer hydrogen bonds and the carboxylate–malonate bridge but their evaluation is precluded by the lack of appropriate models.

The field dependence of the magnetization at 2.0 K, per cobalt(II) ion, of a polycrystalline sample of **1** (see inset of Fig. 3) shows a quasi saturation value (M_S) of 2.25 $N_A\beta$ at 2 K and an applied magnetic field of 5 T. This value is smaller than the calculated M_S value of 3 ($S_{Co} = 3/2$) when $g = 2$. This difference is due to the fact that only the ground Kramers doublet is populated at 2.0 K,[39,45] with an effective spin $S_{eff} = 1/2$ and $g = (10 + 2A\kappa)/3$. For $A = 1.5$ and $\kappa = 0.98$ (see above), $M_S = 2.15\ N_A\beta$, a value which is close to the experimental one.

The thermal dependence of the $\chi_M T$ product [χ_M being the magnetic susceptibility per nickel(II) ion] for compound **2** is shown in Fig. 4. At room temperature, $\chi_M T$ is equal to 1.22 $cm^3\ mol^{-1}$ K, a value which is as expected for a magnetically isolated spin triplet (1.21 $cm^3\ mol^{-1}$ K with $g = 2.20$). Upon cooling, $\chi_M T$ increases reaching a maximum value of 1.34 $cm^3\ mol^{-1}$ K at 7.5 K, and then decreases at lower temperatures. This behaviour is indicative of the occurrence of a very weak ferromagnetic coupling between the Ni(II) ions, the slight decrease in the low temperature range being due single-ion zero-field splitting of the Ni(II) ions (D) and/or very weak antiferromagnetic interactions. The absence of susceptibility maximum in the χ_M *vs.* T plot indicates that the decrease of $\chi_M T$ is mainly due to D. The magnetisation *vs.* H plot at 2.0 K, per nickel(II) ion, of a polycrystalline sample of **2** (see inset of Fig. 4) shows a quasi paramagnetic behaviour, the value of the magnetization at 5 T (the maximum field available in our magnetometer) being 1.65 $N_A\beta$. This value is significantly below that expected for a spin triplet (*ca.* 2.20 $N_A\beta$ with $g = 2.20$), in agreement with the dominant role of the zero-field splitting term at low temperatures and the very weak ferromagnetic coupling observed.

Compound **2** has a two-dimensional and quasi quadratic structure in which the carboxylate–malonate groups act as bridges in the *anti–syn* conformation between the nickel(II) ions. In order to determine the value of the weak ferromagnetic coupling observed in **2**, we have fitted the high temperature magnetic data ($T > 16$ K) of **2** through the high-temperature series expansion derived from the two-dimensional Heisenberg model for a S = 1 manifold ferromagnet square lattice [eqn. (2)],[46] assuming that the two nickel atoms are equivalent.

$$\chi = [Ng^2\beta^2/(3kT)]X\left(1 + \sum_{n=1}^{8} A_n(X)K^n\right) \qquad (2)$$

where

$$A_n(X) = \sum_{i=1}^{n} a_n X^n$$

$$X = S(S+1)$$

and

$$K = J/kT$$

In this expression, the parameters N, g, β and k are the Avogadro's number, Landé factor, Bohr magneton and Boltzman's constant, respectively. A_n and a_n are the coefficients for the square lattice and J is the intralayer magnetic coupling between the local spins of the nearest-neighbours [Hamiltonian of eqn. (3)]

$$H = -J\Sigma_i S_i \cdot S_{i+1} \qquad (3)$$

In this approach, the single-ion zero-field splitting of the Ni(II) ions is not considered, assuming that its effect is not important in the temperature range considered.[47] This expression is valid for systems in which all the nickel(II) ions are equivalent, which is not the case with compound **2**, so we will have an approximate value for J and a mean value for the Landé factor for both nickel(II) ions. The best-fit parameters using a nonlinear regression analysis are: $J = +0.18(2)$ cm^{-1}, $g = 2.20(1)$ and $R = 3.8 \times 10^{-4}$ where R is the agreement factor defined as $\Sigma_i[(\chi_M T)_{obs}(i) - (\chi_M T)_{calc}(i)]^2/\Sigma[(\chi_M T)_{obs}(i)]^2$. The calculated curve matches very well the experimental data in the temperature range 16–295 K.

A literature survey of the magneto-structural data on carboxylate–malonate copper(II) complexes where the carboxylate exhibits the *anti–syn* coordination mode reveals the occurrence of moderate (when linking equatorial positions of adjacent copper atoms) to weak (when linking equatorial and axial positions of adjacent copper atoms) ferromagnetic interactions.[48–50] This ability of the carboxylate group to mediate ferromagnetic interactions between copper(II) ions when acting as a bridge through the *anti–syn* coordination mode has been substantiated by DFT type calculations.[51] The orthogonality between the two copper centred magnetic orbitals (which lie mainly in the equatorial plane of the copper atom) through this carboxylate bridge accounts for the ferromagnetic coupling observed. Although magneto-structural studies on carboxylate-bridged nickel(II) with the carboxylate adopting the *anti–syn* bridging mode are rare, ferromagnetic interactions through this exchange pathway are known.[52] This exchange pathway is most likely responsible for the ferromagnetic coupling observed in **2**, the disagreement between the experimental data and calculated curve in the low temperature range being due to influence of the zero-field splitting and/or very weak antiferromagnetic interactions through hydrogen bonds.

Finally, a point which deserves a brief comment is the fact that the magnetic coupling between the cobalt(II) (**1**) and nickel(II) ions (**2**) through the carboxylate–malonate bridge is antiferro- (**1**) and ferromagnetic (**2**). The different electronic configuration of the metal ions involved with three (**1**) and two

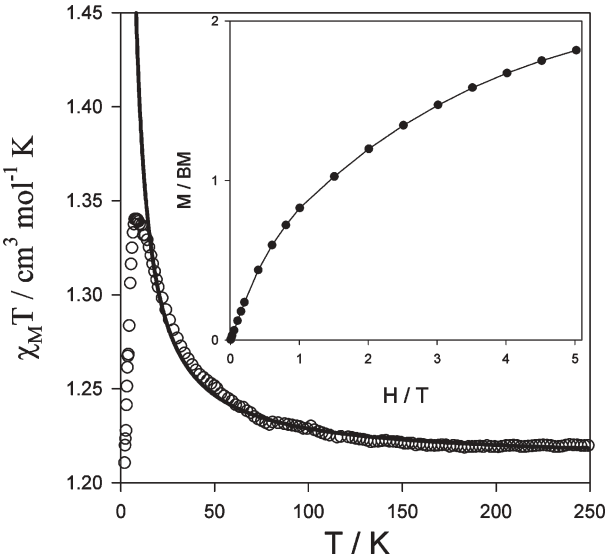

Fig. 4 Thermal dependence of the $\chi_M T$ product for **2** per Ni: (○) experimental; (—) best-fit curve (see text). The inset shows the magnetisation *versus* H plot at 2.0 K for **2**: (○) experimental; (—) eye-guide line.

(**2**) unpaired electrons [$t_{2g}^5e_g^2$ for Co(II) and $t_{2g}^6e_g^2$ for Ni(II), O_h symmetry] would account for that. As the ferromagnetic coupling in **2** is very weak, the presence of one unpaired electron in the t_{2g} type orbital for **1** would increase the possibility of net overlap between the magnetic orbitals,[2] thus enhancing the antiferromagnetic contributions in **1** and the ferromagnetic terms would be overcome. The weak antiferromagnetic coupling observed between the manganese(II) ions [$t_{2g}^3e_g^2$ electronic configuration] bridged by carboxylate–malonate units[13] where the three t_{2g} type orbitals are half filled, gives additional support to this suggestion.

Conclusions

Homometallic malonate-containing complexes with the first-row transition metal ions Co(II), Ni(II), Zn(II) and Mn(II) have 2-D structures exhibiting two different topologies. Co(II), (**1**) Ni(II) (**2**) and Zn(II) malonate complexes are isostructural and their structure exhibits corrugated layers of metal(II) ions bridged through carboxylate–malonate in the *anti–syn* conformation. Coexistence of *anti–syn* and *anti–anti* bridging modes occurs in the case of Mn(II). The reaction of these homometallic malonate complexes with N-exo pyridyl ligands affords two- and three-dimensional structures where malonate-bridged metal(II) layers (*anti–syn* conformation of the carboxylate–malonate) with the same topology are observed, this topology being different from that of the original homometallic malonates, as shown in Scheme 1.

Weak antiferro- (**1**) and ferromagnetic (**2**) interactions between the cobalt(II) (**1**) and nickel(II) (**2**) ions through carboxylate–malonate bridges with the *anti–syn* conformation are observed supporting the ability of the malonate bridge to mediate magnetic interactions between metal ions other than copper(II).

Acknowledgements

We acknowledge financial support from the Ministerio Español de Ciencia y Tecnología (Project BQU2001-3794) and the Consejería de Educación, Cultura y Deportes of Gobierno Autónomo de Canarias (Project PI2002/175). F.S.D. acknowledges the Gobierno Autónomo de Canarias for a pre-doctoral fellowship.

References

1 *Molecule Based Materials*, ed. J. S. Miller and M. Drillon, Wiley-VCH, Weinheim, 2001.
2 O. Kahn, *Molecular Magnetism*, VCH, Weinheim, 1993.
3 M. Pilkington and S. Decurtins, in *Comprehensive Coordination Chemistry II. From Biology to Nanotechnology*, ed. J. A. Mc Cleverty and T. J. Meyer, Elsevier, 2004, **vol. 7**, p. 177.
4 (*a*) M. Verdaguer, A. Bleuzen, V. Marvaud, J. Vaissermann, M. Seuleiman, C. Desplanches, A. Scuiller, C. Train, R. Garde, G. Gelly, C. Lamenech, I. Rosenman, P. Veillet, C. Cartier and F. Villain, *Coord. Chem. Rev.*, 1999, **1023**, 190; (*b*) M. Ohba and H. Okawa, *Coord. Chem. Rev.*, 2000, **198**, 313.
5 J. Ribas, A. Escuer, M. Monfort, R. Vicente, R. Cortés, L. Lezama and T. Rojo, *Coord. Chem. Rev.*, 1999, **193**, 1027.
6 P. Chaudhuri, *Coord, Chem. Rev.*, 2003, **243**, 143.
7 S. R. Batten and K. S. Murray, *Coord. Chem. Rev.*, 2003, **246**, 103.
8 Y. Rodríguez-Martín, M. Hernández-Molina, F. S. Delgado, J. Pasán, C. Ruiz-Pérez, J. Sanchiz, F. Lloret and M. Julve, *CrystEngComm*, 2002, 522.
9 Y. Rodríguez-Martín, M. Hernández-Molina, F. S. Delgado, J. Pasán, C. Ruiz-Pérez, J. Sanchiz, F. Lloret and M. Julve, *CrystEngComm*, 2002, 440.
10 C. Ruiz-Pérez, Y. Rodríguez-Martín, M. Hernández-Molina, F. S. Delgado, J. Pasán, J. Sanchiz, F. Lloret and M. Julve, *Polyhedron*, 2003, **22**, 2111.
11 Y. Rodríguez-Martín, J. Sanchiz, C. Ruiz-Pérez, F. Lloret and M. Julve, *CrystEngComm*, 2002, 631.
12 Y. Rodríguez-Martín, J. Sanchiz, C. Ruiz-Pérez, F. Lloret and M. Julve, *Inorg. Chim. Acta*, 2001, **326**, 20.
13 Y. Rodríguez-Martín, M. Hernández-Molina, J. Sanchiz, C. Ruiz-Pérez, F. Lloret and M. Julve, *Dalton Trans.*, 2003, 2359.
14 S. Konar, P. S. Mukherjee, M. G. B. Drew, J. Ribas and N. R. Chaudhuri, *Inorg. Chem.*, 2003, **42**, 2545.
15 F. S. Delgado, J. Sanchiz, C. Ruiz-Pérez, F. Lloret and M. Julve, *Inorg. Chem.*, 2003, **42**, 5938.
16 T. F. Liu, H. L. Sun, S. Gao, S. W. Zhang and T. C. Lau, *Inorg. Chem.*, 2003, **42**, 4792.
17 F. S. Delgado, J. Sanchiz, C. Ruiz-Pérez, F. Lloret and M. Julve, *CrystEngComm*, 2003, 280.
18 C. Ruiz-Pérez, J. Sanchiz, M. H. Molina, F. Lloret and M. Julve, *Inorg. Chem.*, 2000, **39**, 1363.
19 D. Chattopadhyay, S. K. Chattopadhyay, P. R. Lowe, C. H. Schwalbe, S. K. Mazumder, A. Rana and S. Ghosh, *J. Chem. Soc., Dalton Trans.*, 1993, 913.
20 N. J. Ray, *Acta Crystallogr., Sect. B*, 1982, **38**, 770.
21 T. Lis and J. Matuszewski, *Acta Crystallogr., Sect. B*, 1979, **35**, 2212.
22 L. Walter-Levy, J. Perrotey and J. W. Visser, *Bull. Soc. Chim. Fr.*, 1973, 2596.
23 A. Earnshaw, *Introduction to Magnetochemistry*, Academic Press, London, 1968.
24 L. J. Farrugia, *J. Appl. Crystallogr.*, 1999, **32**, 837.
25 G. M. Sheldrick, SHELXS-97 & SHELXL-97, Programs for Crystal Structure Anlysis (Release 97-2), Institut für Anorganische Chemie der Universität, Tammanstrasse 4, D-3400 Göttingen, Germany, 1998.
26 M. Nardelli, *J. Appl. Crystallogr.*, 1995, **28**.
27 Crystal Maker 4.2.1. Crystalmaker Sofware., P.O. Box 183, Bicester, Oxfordshire, OX26 3TA, UK, 2001.
28 E. I. Stiefel and G. F. Brown, *Inorg. Chem.*, 1972, **2**, 434.
29 D. Cremer and J. A. Pople, *J. Am. Chem. Soc.*, 1975, **97**, 1354.
30 Z.-X. Wang, X.-H. Zhou, W.-T. Yu and Y.-J. Fu, *Z. Kristallogr. - New Cryst. Struct.*, 2000, **215**, 423.
31 T. K. Maji, S. Sain, G. Mostafa, T.-H. Lu, J. Ribas, M. Monfort and N. R. Chaudhuri, *Inorg. Chem.*, 2003, **42**, 709.
32 L. Shen, *Acta Crystallogr., Sect. C*, 2003, **59**, m128.
33 X. T. Zhang, C. Z. Lu, Q. Z. Zhang, S. F. Lu, W. B. Yang, J. C. Liu and H. H. Zhuang, *Eur. J. Inorg. Chem.*, 2003, 1181.
34 A. D. Burrows, R. W. Harrington, M. F. Mahon and C. E. Price, *Dalton Trans.*, 2000, 3845.
35 P. Lightfoot and A. Snedden, *Dalton Trans.*, 1999, 3549.
36 F. S. Delgado, J. Sanchiz, C. Ruiz-Pérez, F. Lloret and M. Julve, unpublished results. .
37 Y.-H. Xue, D.-D. Lin and D.-J. Xu, *Acta Crystallogr., Sect. E*, 2004, **59**, m750.
38 D.-D. Lin, Y. Liu and D.-J. Xu, *Acta Crystallogr., Sect. E*, 2004, **59**, m771.
39 R. L. Carlin, *Magnetochemistry*, Springer-Verlag, Berlin, Heidelberg, 1986.
40 F. E. Mabbs and D. J. Machin, *Magnetism and Transition Metal Complexes*, Chapman and Hall Ltd., London, 1973.
41 H. Kumagai, Y. Oka, K. Inoue and M. Kurmoo, *Dalton Trans.*, 2002, 3442.
42 E. W. Lee, Y. J. Kim and D. K. Jung, *Inorg. Chem.*, 2002, **41**, 501.
43 J. M. Rueff, N. Masciocchi, P. Rabu, A. Sironi and A. Skoulios, *Eur. J. Inorg. Chem.*, 2001, 2843.
44 J. M. Herrera, A. Bleuzen, Y. Dromzée, M. Julve, F. Lloret and M. Verdaguer, *Inorg. Chem.*, 2003, **42**, 7052.
45 E. Coronado, M. Drillon, P. R. Nutgeren, L. J. De Jongh and D. Beltrán, *J. Am. Chem. Soc.*, 1988, **110**, 3907.
46 R. Navarro, *Application of High- and Low-Temperature Series Expansions to Two-Dimensional Magnetic Systems*, ed.L. J. de Jongh, Kluwer Academic Publishers, Dordrecht, 1990.
47 O. Castillo, A. Luque, P. Román, F. Lloret and M. Julve, *Inorg. Chem.*, 2001, **40**, 5526.
48 J. Pasán, F. S. Delgado, Y. Rodríguez-Martín, M. Hernández-Molina, C. Ruiz-Pérez, J. Sanchiz, F. Lloret and M. Julve, *Polyhedron*, 2003, **22**, 2143.
49 F. S. Delgado, J. Sanchiz, C. Ruiz-Pérez, F. Lloret and M. Julve, *Inorg. Chem.*, 2003, **42**, 5938.
50 J. Pasán, J. Sanchiz, C. Ruiz-Pérez, F. Lloret and M. Julve, *New J. Chem.*, 2003, **27**, 1557.
51 A. Rodríguez-Fortea, P. Alemany, S. Álvarez and E. Ruiz, *Chem. Eur. J.*, 2001, **7**, 627.
52 T. Whitfield, L. M. Zheng, X. Wang and A. J. Jacobson, *Solid State Sci.*, 2001, **3**, 829.